Kaon Spectroscopy at COMPASS

Boris Grube

Thomas Jefferson National Accelerator Facility

KLF Collaboration Meeting

September 19, 2023

Jefferson Lab, Newport News, VA

Why Kaon Spectroscopy?

PDG 2022: 25 Kaon States

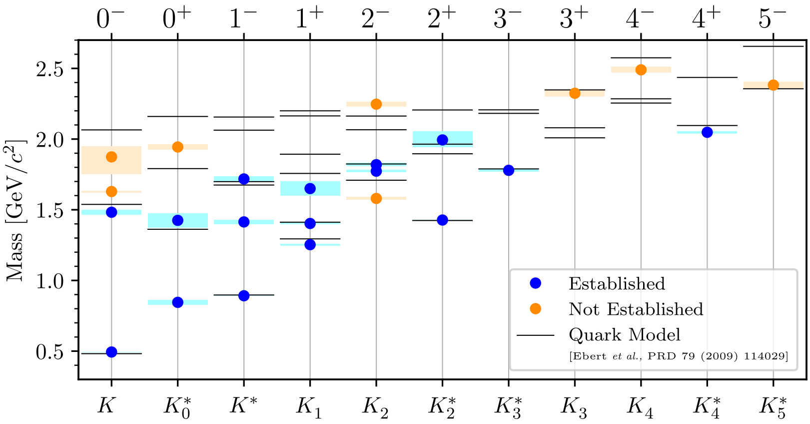

[Courtesy S. Wallner, TUM]

- Only 16 kaon states well established
- 9 states need confirmation
- Many PDG entries more than 30 years old
- Many predicted quark-model states still missing
- Some hints for supernumerary states
  $\Longrightarrow$ non-$q\bar{q}$ states?

Why Kaon Spectroscopy?

PDG 2022: 25 Kaon States

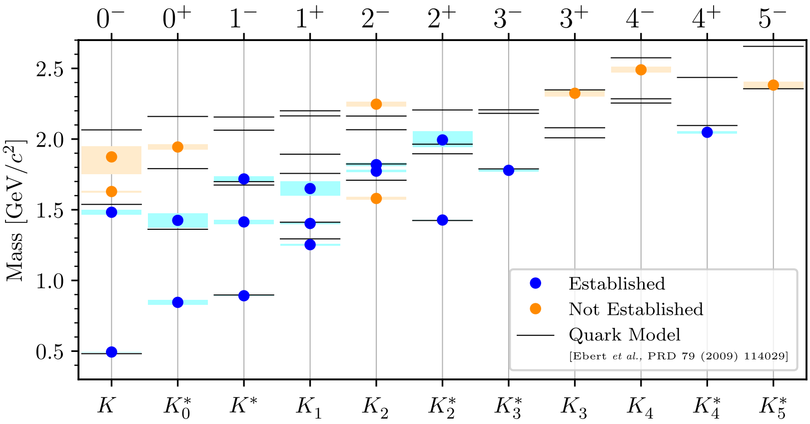

[Courtesy S. Wallner, TUM]

- Only 16 kaon states well established
- 9 states need confirmation
- Many PDG entries more than 30 years old
- Many predicted quark-model states still missing
- Some hints for supernumerary states
  $\Longrightarrow$ non-$q\bar{q}$ states?

Why Kaon Spectroscopy?

Kaon spectrum crucial to understand light-meson spectrum

- Identify supernumerary states by completing SU(3)$_{\text{flavor}}$ multiplets
  - E.g. $J^P = 0^+$ nonet with $a_0(980)$, $K_0^*(700)$ [or κ], $f_0(500)$ [or σ], and $f_0(980)$ is hypothesized to be tetra-quark multiplet
  - Only since PDG 2021 $K_0^*(700)$ is “well established”

Kaon spectrum required as input in other fields

- E.g. search for CP violation in multi-body decays of heavy mesons
  - *Example:* $B^\pm \to D^0 K^\pm$ with $D^0 \to K_S^0 \pi^+ \pi^-$
  - Amplitude analysis of D^0 Dalitz plot requires accurate knowledge of resonances in $K_S^0 \pi^\pm$ and $\pi^+ \pi^-$ subsystems

Kaon spectrum crucial to understand light-meson spectrum

- Identify supernumerary states by completing SU(3)$_{\text{flavor}}$ multiplets
  - E.g. $J^P = 0^+$ nonet with $a_0(980)$, $K_0^*(700)$ [or κ], $f_0(500)$ [or σ], and $f_0(980)$ is hypothesized to be tetra-quark multiplet
  - Only since PDG 2021 $K_0^*(700)$ is “well established”

Kaon spectrum required as input in other fields

- E.g. search for CP violation in multi-body decays of heavy mesons
  - *Example:* $B^\pm \to D^0 K^\pm$ with $D^0 \to K_S^0 \pi^+ \pi^-$
  - Amplitude analysis of D^0 Dalitz plot requires accurate knowledge of resonances in $K_S^0 \pi^\pm$ and $\pi^+ \pi^-$ subsystems

Kaon Spectroscopy at COMPASS

Main Production Process: Diffractive Dissociation

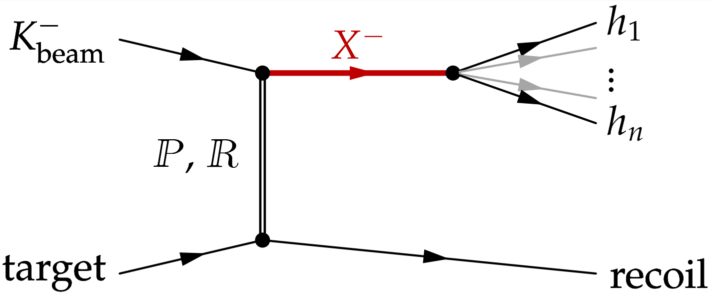

- 190 GeV/c kaon beam on stationary proton or nuclear target
- Triggering on target recoil ensures elastic scattering at target vertex
- Highly excited states prefer to decay into multi-body hadronic final states
- Various final states measurable
- n-body final state strongly boosted $\Longrightarrow$ forward spectrometer

Multi-purpose fixed-target experiment

- Beam-particle ID (CEDARs)
- Two-stage spectrometer
- High-precision measurement of charged-particle trajectories
- Detectors for energy measurement and particle identification
- 1 PB of data per year

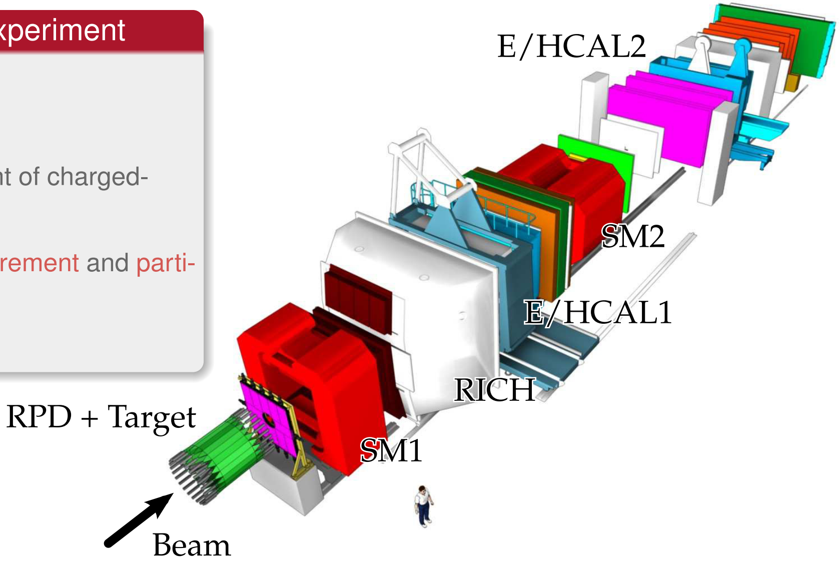

Golden Channel: Diffractive $K^-\pi^-\pi^+$ Production

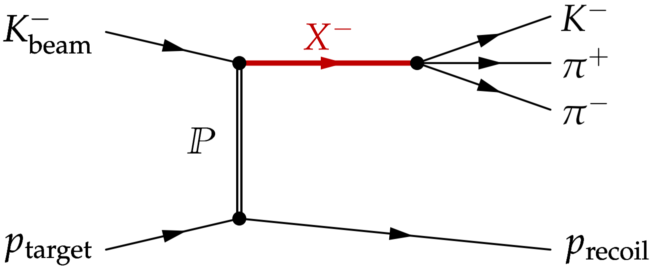

- All kaon states (except $J^P = 0^+$) can appear as intermediate states X^-
- Study several decay modes over wide mass range in single analysis, e.g.
  - $X^- \to \rho(770)\,K^-,\ f_2(1270)\,K^-, \ldots$
  - $X^- \to K^*(892)\,\pi^-,\ K_2^*(1430)\,\pi^-, \ldots$
- Strange partner process to $\pi^- + p \to \pi^-\pi^-\pi^+ + p$
  - Studied in great detail at COMPASS

    PRL **115** (2015) 082001; PRD **95** (2017) 032004; PRD **98** (2018) 092003; PRD **105** (2022) 012005

Golden Channel: Diffractive $K^- \pi^- \pi^+$ Production

190 GeV/c K^- beam on p target

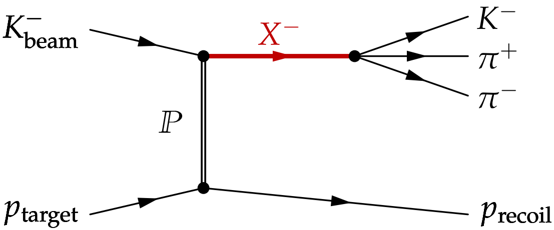

- Beam contains 2.4 % K^-
- World's largest sample: 720k exclusive events
- $0.1 < t' < 1.0\,(\text{GeV}/c)^2$
- Potential resonance signals
  - Disentangled using partial-wave analysis (PWA) techniques
- $\approx 3.5\times$ more data than CERN WA03

Golden Channel: Diffractive $K^-\pi^-\pi^+$ Production

190 GeV/c K^- beam on p target

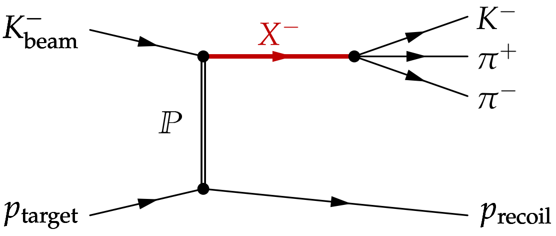

- Beam contains 2.4 % K^-
- World's largest sample: 720k exclusive events
- $0.1 < t' < 1.0\,(\text{GeV}/c)^2$
- Potential resonance signals
  - Disentangled using partial-wave analysis (PWA) techniques
- $\approx 3.5\times$ more data than CERN WA03

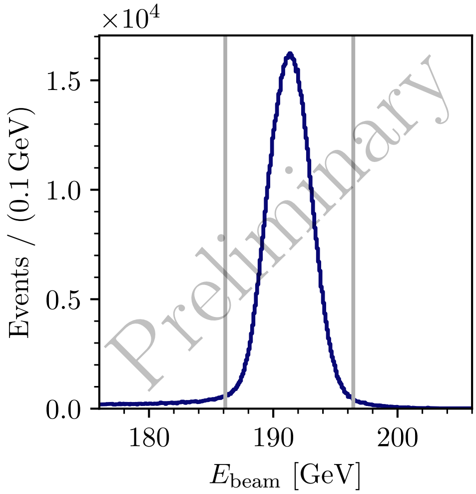

Golden Channel: Diffractive $K^-\pi^-\pi^+$ Production

190 GeV/c K^- beam on p target

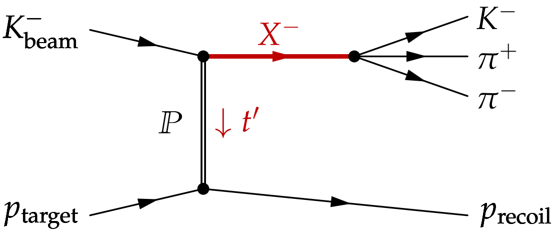

- Beam contains 2.4 % K^-
- World's largest sample: 720k exclusive events
- $0.1 < t' < 1.0$ (GeV/c)^2
- Potential resonance signals
  - Disentangled using partial-wave analysis (PWA) techniques
- $\approx 3.5\times$ more data than CERN WA03

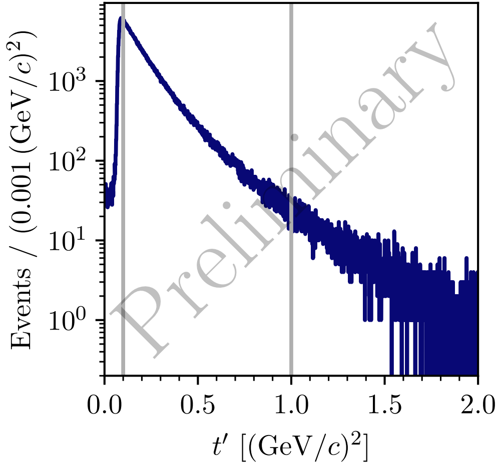

Golden Channel: Diffractive $K^- \pi^- \pi^+$ Production

190 GeV/c K^- beam on p target

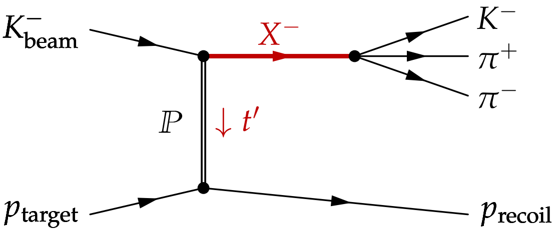

- Beam contains 2.4 % K^-
- World's largest sample: 720k exclusive events
- $0.1 < t' < 1.0\,(\text{GeV}/c)^2$
- Potential resonance signals
  - Disentangled using partial-wave analysis (PWA) techniques
- $\approx 3.5\times$ more data than CERN WA03

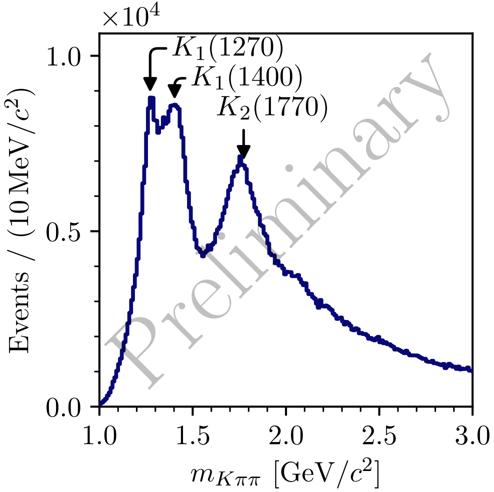

Golden Channel: Diffractive $K^-\pi^-\pi^+$ Production

190 GeV/c K^- beam on p target

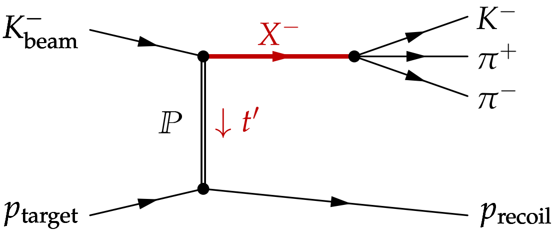

- Beam contains 2.4 % K^-
- World's largest sample: 720k exclusive events
- $0.1 < t' < 1.0\,(\text{GeV}/c)^2$
- Potential resonance signals
  - Disentangled using partial-wave analysis (PWA) techniques
- $\approx 3.5\times$ more data than CERN WA03

200k events, $0 < t' < 0.7\,(\text{GeV}/c)^2$

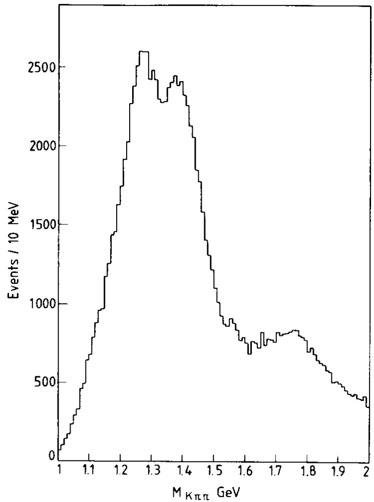

ACCMOR, NPB **187** (1981) 1

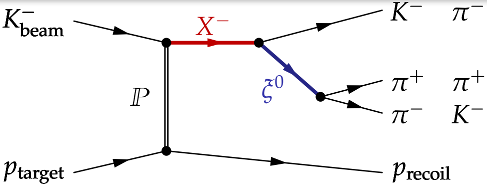

- X^- decays via $\pi^- \pi^+$ and $K^- \pi^+$ "isobar" resonances ξ^0
- J^P of a resonance determines angular distribution of its daughter particles
- *Analogy:* multipole radiation in classical electrodynamics
- Determine J^P of intermediate resonances X^- and ξ^0 from measured angular distribution of final-state particles

Partial-Wave Analysis of $K^- \pi^- \pi^+$

Isobar Model

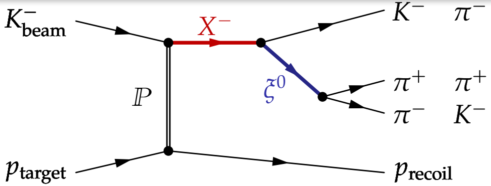

- X^- decays via $\pi^-\pi^+$ and $K^-\pi^+$ "isobar" resonances ξ^0
- J^P of a resonance determines angular distribution of its daughter particles
- *Analogy:* multipole radiation in classical electrodynamics
- Determine J^P of intermediate resonances X^- and ξ^0 from measured angular distribution of final-state particles

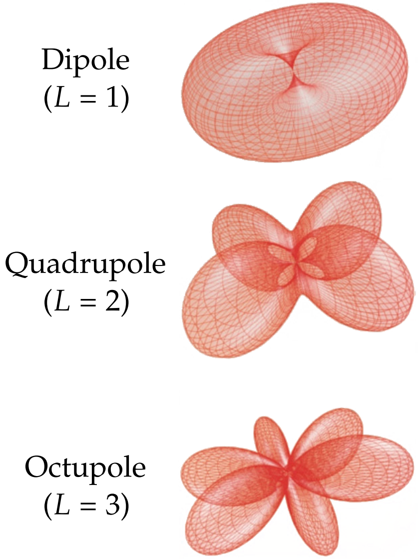

Partial-Wave Analysis of $K^- \pi^- \pi^+$

Isobar Model

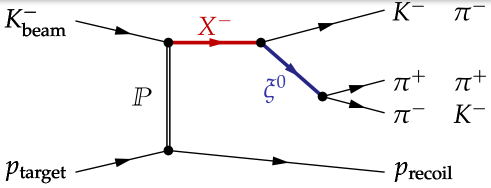

- X^- decays via $\pi^-\pi^+$ and $K^-\pi^+$ "isobar" resonances ξ^0
- J^P of a resonance determines angular distribution of its daughter particles
- *Analogy:* multipole radiation in classical electrodynamics
- Determine J^P of intermediate resonances X^- and ξ^0 from measured angular distribution of final-state particles

Dipole ($L = 1$)

Quadrupole ($L = 2$)

Octupole ($L = 3$)

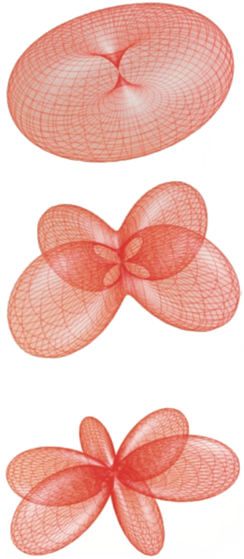

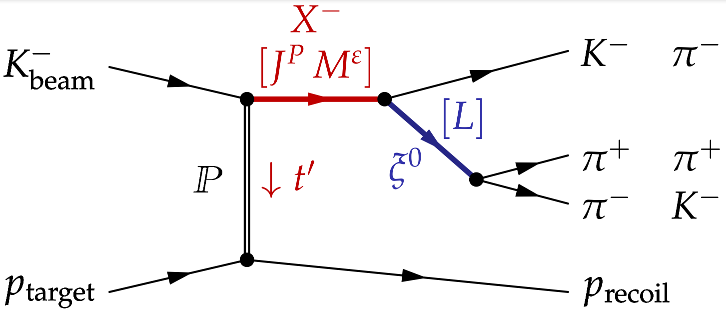

Partial wave defined by

- $J^P M^\varepsilon$ quantum numbers of X^-
- Orbital angular momentum L between ξ^0 and bachelor π^-/K^-
- Isobar resonance ξ^0
- *Example:* $1^+ 0^+ \rho(770) K S$

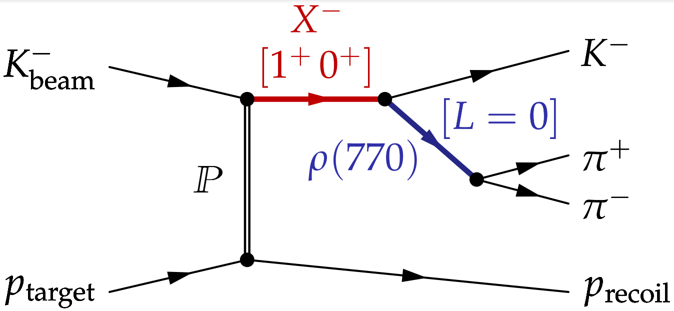

Partial wave defined by

- $J^P M^\varepsilon$ quantum numbers of X^-
- Orbital angular momentum L between ξ^0 and bachelor π^-/K^-
- Isobar resonance ξ^0
- *Example:* $1^+ 0^+ \rho(770) K S$

Partial-Wave Analysis of $K^-\pi^-\pi^+$

First Analysis Stage: Partial-Wave Decomposition in $(m_{K\pi\pi}, t')$ Cells

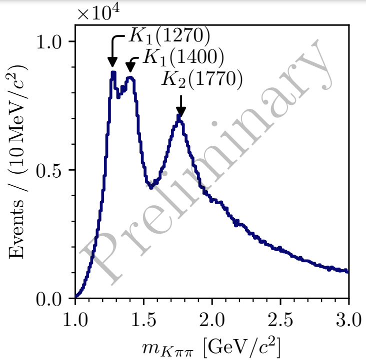

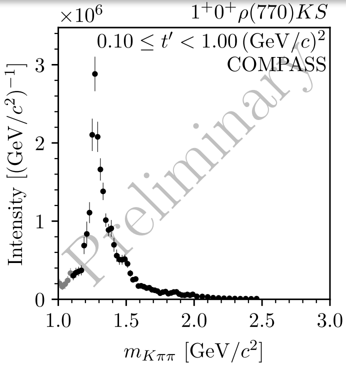

- Fit PWA model to data in $(m_{K\pi\pi}, t')$ cells $\Longrightarrow$ partial-wave amplitudes in each cell
- Wave set inferred from data using regularization-based model-selection techniques
- Uncertainties estimated by boostrapping
- Verified method by performing detailed Monte Carlo input-output studies

Partial-Wave Analysis of $K^- \pi^- \pi^+$

Second Analysis Stage: Resonance-Model Fit

- Model $m_{K\pi\pi}$ dependence of partial-wave amplitudes
- Resonance components modeled using Breit-Wigner amplitudes
- Coherent non-resonant component
- Incoherent backgrounds from other processes
  - Incoherent background from $\pi^- \, p \to \pi^- \pi^- \pi^+ \, p$ explicitly modeled using results from $\pi^- \pi^- \pi^+$ PWA
  - Incoherent effective background component models other background processes

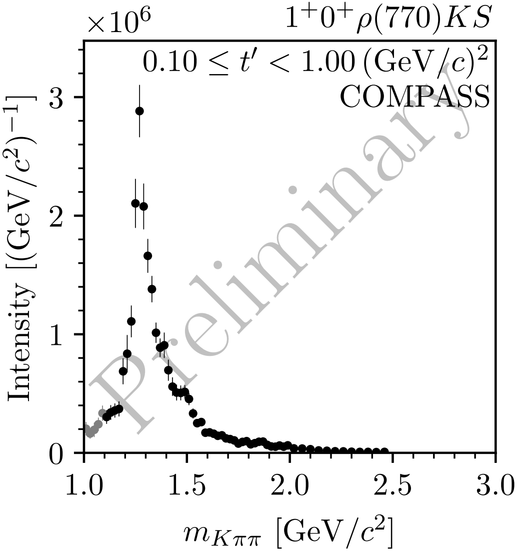

Partial-Wave Analysis of $K^- \pi^- \pi^+$

Second Analysis Stage: Resonance-Model Fit

- Model $m_{K\pi\pi}$ dependence of partial-wave amplitudes
- Resonance components modeled using Breit-Wigner amplitudes
- Coherent non-resonant component
- Incoherent backgrounds from other processes
  - Incoherent background from $\pi^- p \to \pi^- \pi^- \pi^+ p$ explicitly modeled using results from $\pi^- \pi^- \pi^+$ PWA
  - Incoherent effective background component models other background processes

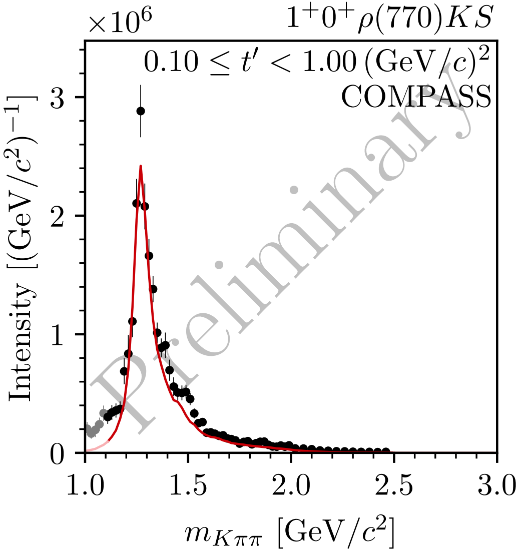

Partial-Wave Analysis of $K^-\pi^-\pi^+$

Second Analysis Stage: Resonance-Model Fit

- Model $m_{K\pi\pi}$ dependence of partial-wave amplitudes
- Resonance components modeled using Breit-Wigner amplitudes
- Coherent non-resonant component
- Incoherent backgrounds from other processes
  - Incoherent background from $\pi^- p \to \pi^-\pi^-\pi^+ p$ explicitly modeled using results from $\pi^-\pi^-\pi^+$ PWA
  - Incoherent effective background component models other background processes

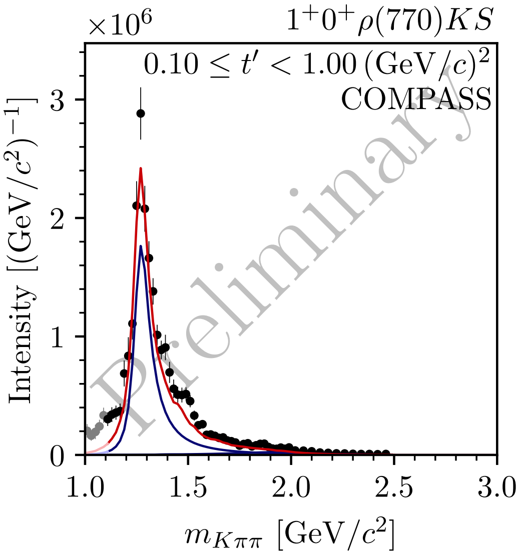

Partial-Wave Analysis of $K^- \pi^- \pi^+$

Second Analysis Stage: Resonance-Model Fit

- Model $m_{K\pi\pi}$ dependence of partial-wave amplitudes
- Resonance components modeled using Breit-Wigner amplitudes
- Coherent non-resonant component
- Incoherent backgrounds from other processes
  - Incoherent background from $\pi^- \, p \to \pi^- \pi^- \pi^+ \, p$ explicitly modeled using results from $\pi^- \pi^- \pi^+$ PWA
  - Incoherent effective background component models other background processes

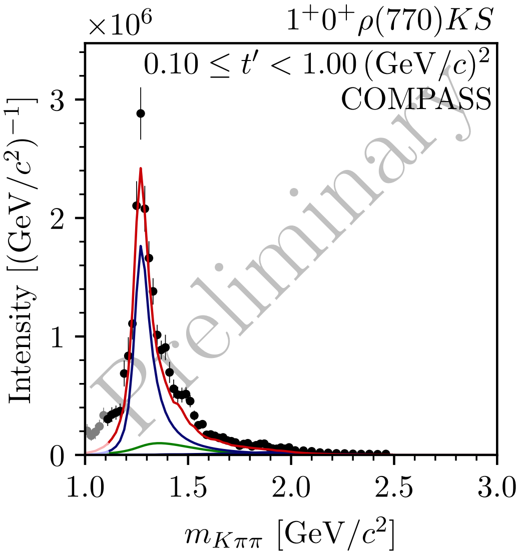

Partial-Wave Analysis of $K^-\pi^-\pi^+$

Second Analysis Stage: Resonance-Model Fit

- Model $m_{K\pi\pi}$ dependence of partial-wave amplitudes
- Resonance components modeled using Breit-Wigner amplitudes
- Coherent non-resonant component
- Incoherent backgrounds from other processes
  - Incoherent background from $\pi^- \; p \to \pi^-\pi^-\pi^+ \; p$ explicitly modeled using results from $\pi^-\pi^-\pi^+$ PWA
  - Incoherent effective background component models other background processes

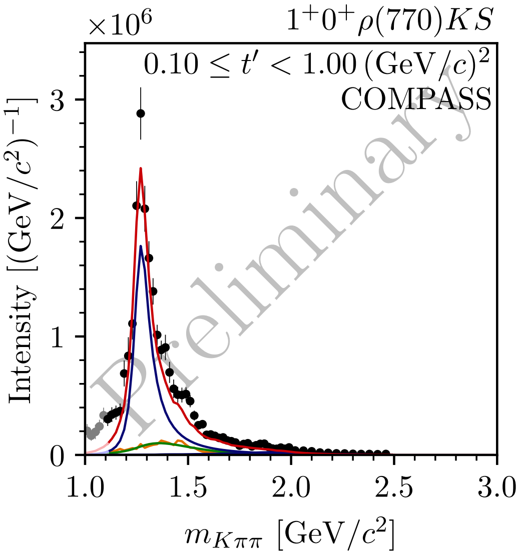

Partial-Wave Analysis of $K^- \pi^- \pi^+$

Second Analysis Stage: Resonance-Model Fit

- Model $m_{K\pi\pi}$ dependence of partial-wave amplitudes
- Resonance components modeled using Breit-Wigner amplitudes
- Coherent non-resonant component
- Incoherent backgrounds from other processes
  - Incoherent background from $\pi^- \; p \to \pi^- \pi^- \pi^+ \; p$ explicitly modeled using results from $\pi^- \pi^- \pi^+$ PWA
  - Incoherent effective background component models other background processes

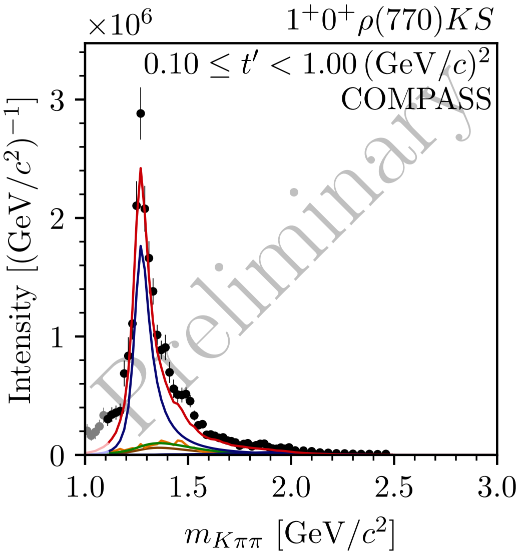

Most comprehensive analysis so far

- Fit amplitudes of 14 waves simultaneously
- Use information from partial-wave intensities and interference terms (relative phases)
- Amplitudes modeled using 13 kaon resonances
- Fit data from 4 t' bins simultaneously
  - Enforcing identical resonance parameters in each t' bin
- 408 fit parameters (11 masses and widths) constrained by 12 768 data points

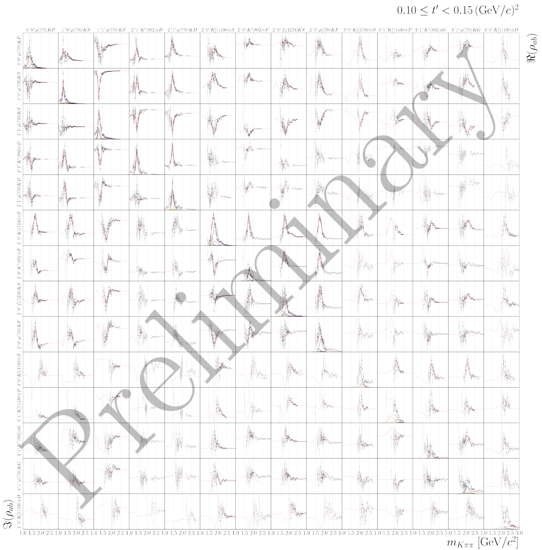

Partial-Wave Analysis of $K^-\pi^-\pi^+$

Second Analysis Stage: Resonance-Model Fit

Most comprehensive analysis so far

- Fit amplitudes of 14 waves simultaneously
- Use information from partial-wave intensities and interference terms (relative phases)
- Amplitudes modeled using 13 kaon resonances
- Fit data from 4 t' bins simultaneously
  - Enforcing identical resonance parameters in each t' bin
- 408 fit parameters (11 masses and widths) constrained by 12 768 data points

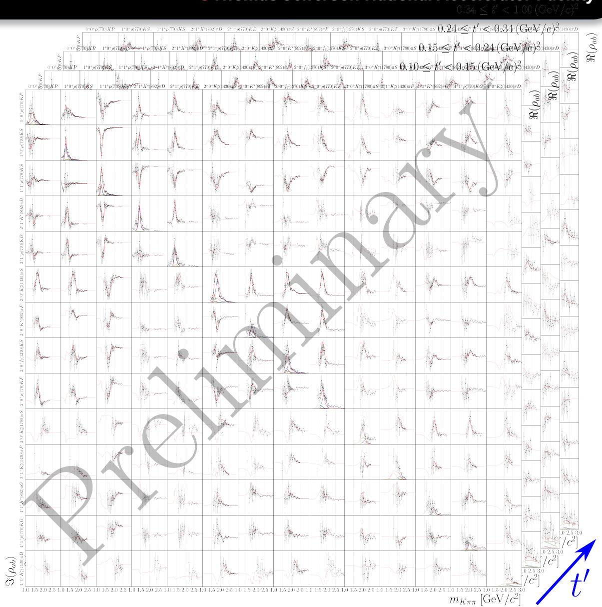

Partial Waves with $J^P = 2^+$

PDG 2022

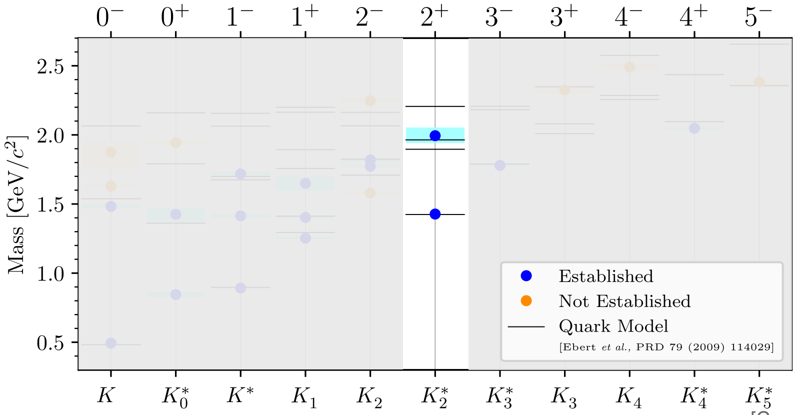

[Courtesy S. Wallner, TUM]

- $K_2^*(1430)$ is well-known resonance

Partial Waves with $J^P = 2^+$

- Observed in two decay modes
  - $\rho(770)\,K\,D$-wave
  - $K^*(892)\,\pi\,D$-wave
- $K_2^*(1430)$ Breit-Wigner parameters
  - $m_0 = 1430.9 \pm 1.4\,(\text{stat.})\,^{+3.1}_{-1.5}\,(\text{sys.})$ MeV/c^2
  - $\Gamma_0 = 111 \pm 3\,(\text{stat.})\,^{+4}_{-16}\,(\text{sys.})$ MeV/c^2
  - In agreement with previous measurements

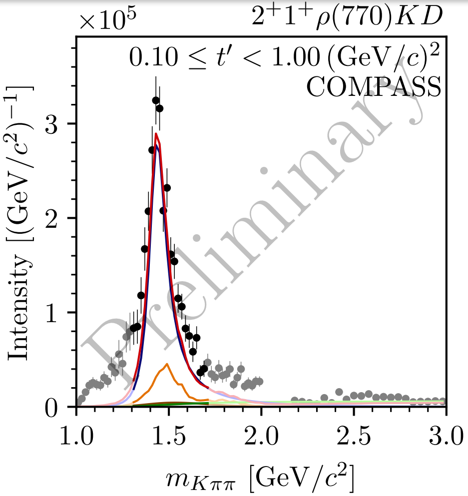

Total model, resonances, $K^-\pi^-\pi^+$ non-resonant, $\pi^-\pi^-\pi^+$ background, other backgrounds

Partial Waves with $J^P = 2^+$

- Observed in two decay modes
  - $\rho(770)\,K\;D$-wave
  - $K^*(892)\,\pi\;D$-wave
- $K_2^*(1430)$ Breit-Wigner parameters
  - $m_0 = 1430.9 \pm 1.4\,\text{(stat.)}\,^{+3.1}_{-1.5}\,\text{(sys.)}\;\text{MeV}/c^2$
  - $\Gamma_0 = 111 \pm 3\,\text{(stat.)}\,^{+4}_{-16}\,\text{(sys.)}\;\text{MeV}/c^2$
  - In agreement with previous measurements

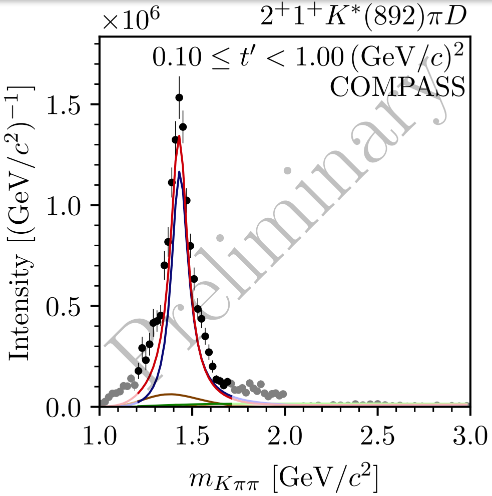

Total model, resonances, $K^-\pi^-\pi^+$ non-resonant, $\pi^-\pi^-\pi^+$ background, other backgrounds

Partial Waves with $J^P = 2^+$

- Observed in two decay modes
  - $\rho(770)\,K\,D$-wave
  - $K^*(892)\,\pi\,D$-wave
- $K_2^*(1430)$ Breit-Wigner parameters
  - $m_0 = 1430.9 \pm 1.4\,\text{(stat.)}\,^{+3.1}_{-1.5}\,\text{(sys.)}\,\text{MeV}/c^2$
  - $\Gamma_0 = 111 \pm 3\,\text{(stat.)}\,^{+4}_{-16}\,\text{(sys.)}\,\text{MeV}/c^2$
  - In agreement with previous measurements

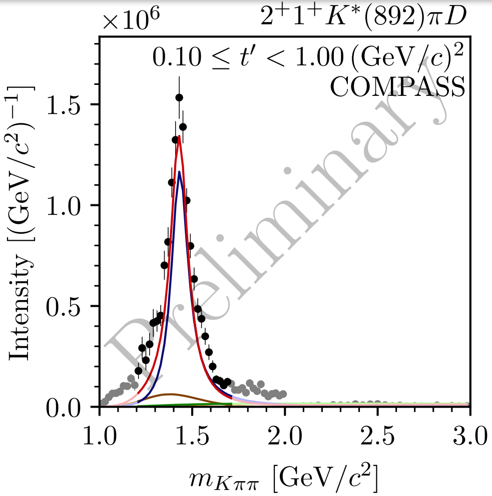

Total model, resonances, $K^-\pi^-\pi^+$ non-resonant, $\pi^-\pi^-\pi^+$ background, other backgrounds

Partial Waves with $J^P = 2^-$

PDG 2022

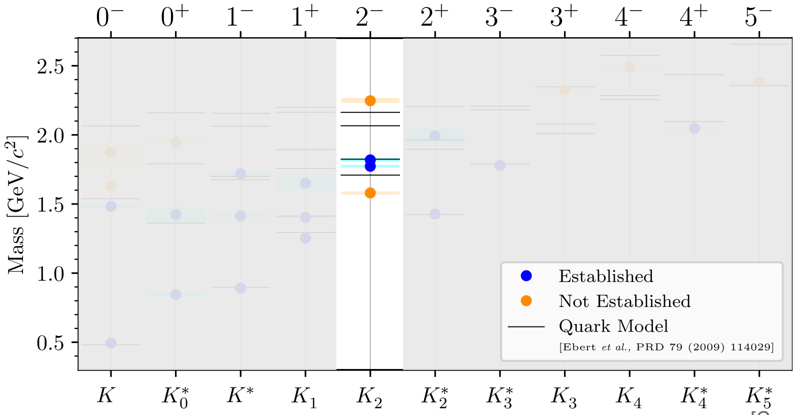

[Courtesy S. Wallner, TUM]

- $K_2(1770)$ and $K_2(1820)$ are established
- $K_2(2250)$ needs further confirmation

Partial Waves with $J^P = 2^-$

- Fitted in 4 decay modes
  - $K^*(892)\,\pi\,F$-wave
  - $\rho(770)\,K\,F$-wave
  - $K_2^*(1430)\,\pi\,S$-wave
  - $f_2(1270)\,K\,S$-wave
- Peak at 1.8 GeV/c^2 described by interference of $K_2(1770)$ and $K_2(1820)$
- High-mass shoulder modeled by $K_2(2250)$
- Different intensity distributions and large phase motions among 2^- waves

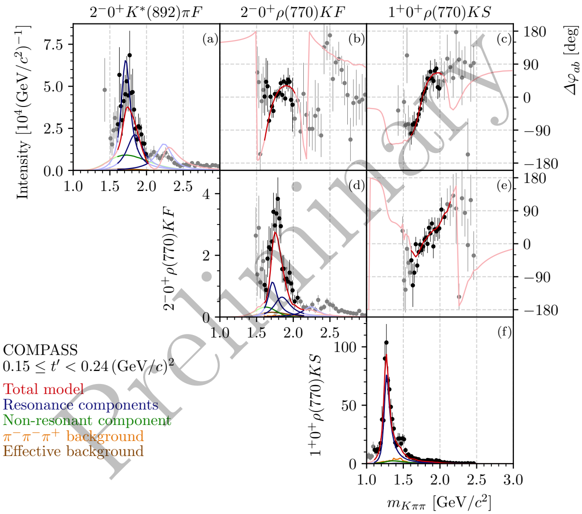

Partial Waves with $J^P = 2^-$

- Fitted in 4 decay modes
  - $K^*(892)\,\pi$ F-wave
  - $\rho(770)\,K$ F-wave
  - $K_2^*(1430)\,\pi$ S-wave
  - $f_2(1270)\,K$ S-wave
- Peak at 1.8 GeV/c^2 described by interference of $K_2(1770)$ and $K_2(1820)$
- High-mass shoulder modeled by $K_2(2250)$
- Different intensity distributions and large phase motions among 2^- waves

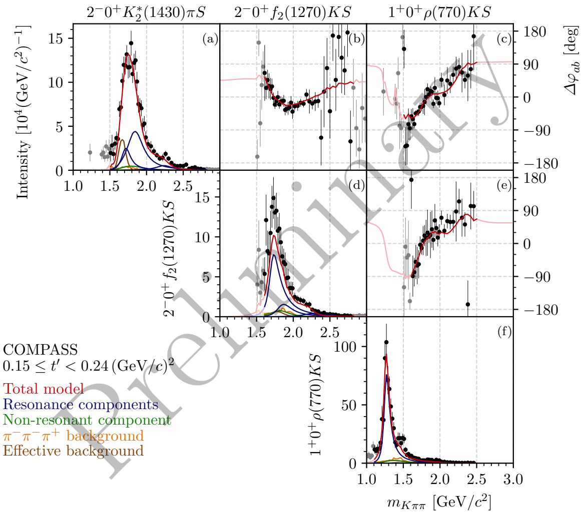

Partial Waves with $J^P = 2^-$

- Fitted in 4 decay modes
  - $K^*(892)\,\pi\,F$-wave
  - $\rho(770)\,K\,F$-wave
  - $K_2^*(1430)\,\pi\,S$-wave
  - $f_2(1270)\,K\,S$-wave
- Peak at 1.8 GeV/c^2 described by interference of $K_2(1770)$ and $K_2(1820)$
- High-mass shoulder modeled by $K_2(2250)$
- Different intensity distributions and large phase motions among 2^- waves

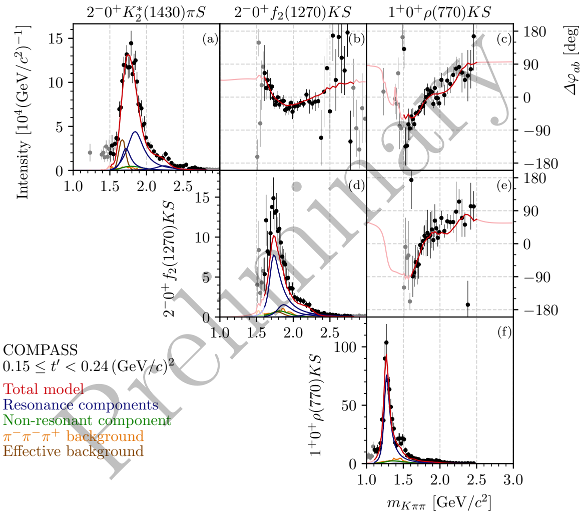

Partial Waves with $J^P = 2^-$

$K_2(1770)$ and $K_2(1820)$

ACCMOR: $K^\pm p \to K^\pm \pi^- \pi^+ p$

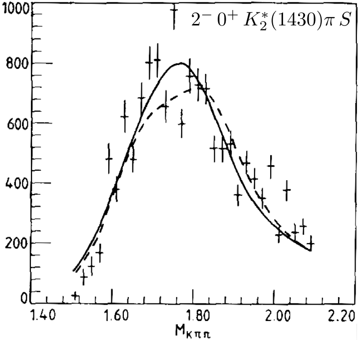

NPB **187** (1981) 1

LASS: $K^- p \to K^- \omega(782)\, p$

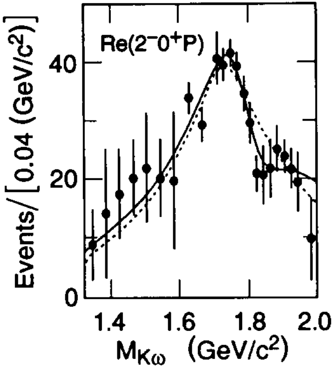

PLB **308** (1993) 186

LHCb: $B^+ \to J/\psi \phi K^+$

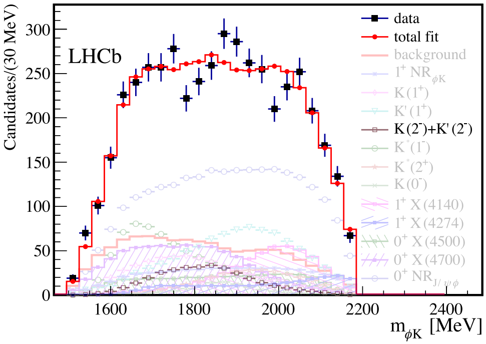

PRL **118** (2017) 022003

- $K_2(1770)$ **and** $K_2(1820)$ considered only in 3 previous analyses
- Only LHCb could confirm 2 states with 3σ significance
- COMPASS observes 2 states with 11σ statistical significance

Partial Waves with $J^P = 2^-$

$K_2(1770)$ and $K_2(1820)$

Jefferson Lab
Thomas Jefferson National Accelerator Facility

ACCMOR: $K^\pm p \to K^\pm \pi^- \pi^+ p$

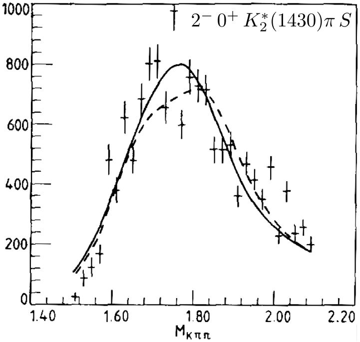

NPB **187** (1981) 1

LASS: $K^- p \to K^- \omega(782)\, p$

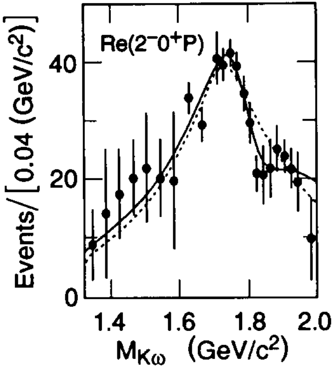

PLB **308** (1993) 186

LHCb: $B^+ \to J/\psi \phi K^+$

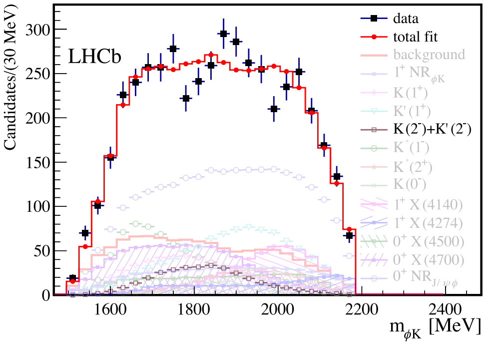

PRL **118** (2017) 022003

- $K_2(1770)$ **and** $K_2(1820)$ considered only in 3 previous analyses
- Only LHCb could confirm 2 states with 3σ significance
- COMPASS observes 2 states with 11σ statistical significance

Partial Waves with $J^P = 2^-$

$K_2(1770)$ and $K_2(1820)$

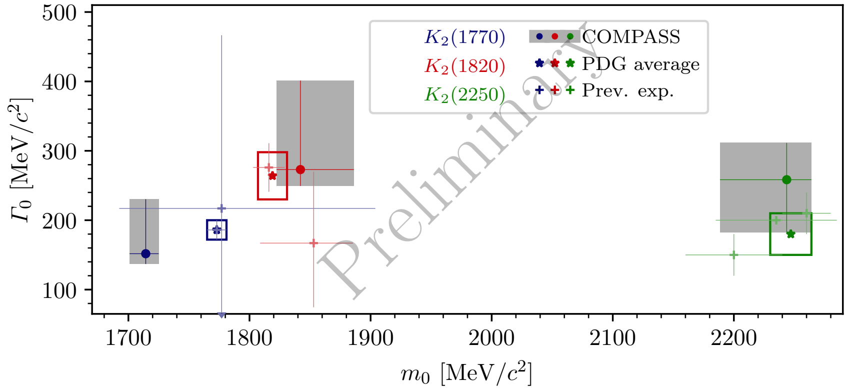

- $K_2(1770)$ **and** $K_2(1820)$ considered only in 3 previous analyses
- Only LHCb could confirm 2 states with 3σ significance
- COMPASS observes 2 states with 11σ statistical significance

Partial Waves with $J^P = 2^-$

$K_2(1770)$, $K_2(1820)$, and $K_2(2250)$

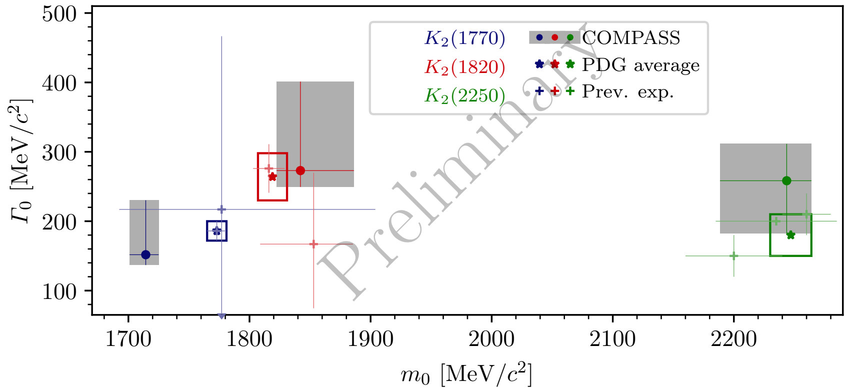

- $K_2(2250)$ so far studied mainly in $\Lambda\bar{p}$ and $\overline{\Lambda}p$ decay channel
- COMPASS: first simultaneous measurement of $K_2(1770)$, $K_2(1820)$, and $K_2(2250)$
- $K_2(2250)$ parameters consistent with previous measurements

Partial Waves with $J^P = 2^-$

$K_2(1770)$, $K_2(1820)$, and $K_2(2250)$

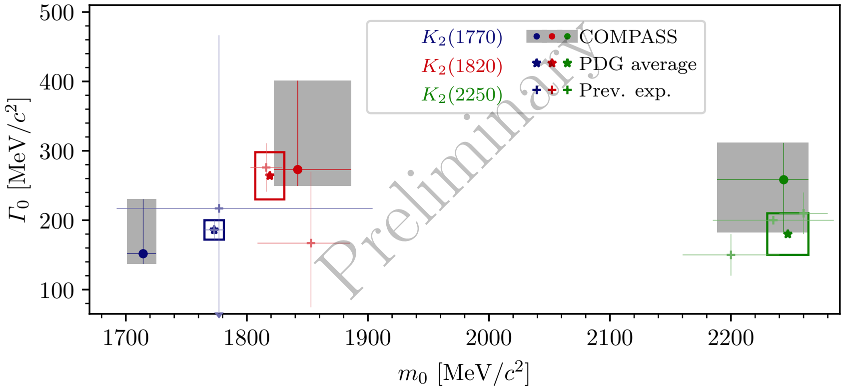

- $K_2(2250)$ so far studied mainly in $\Lambda\bar{p}$ and $\overline{\Lambda}p$ decay channel
- COMPASS: first simultaneous measurement of $K_2(1770)$, $K_2(1820)$, and $K_2(2250)$
- $K_2(2250)$ parameters consistent with previous measurements

Partial Waves with $J^P = 0^-$

PDG 2022

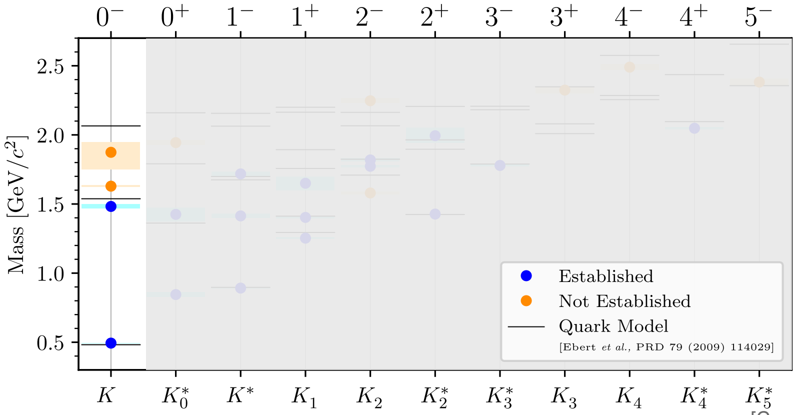

[Courtesy S. Wallner, TUM]

- $K(1460)$ is established
- $K(1630)$ and $K(1830)$ need confirmation

- $K(1630)$ seen by only one experiment
  - Width is only 16 MeV/c^2
  - Unknown J^P

Partial Waves with $J^P = 0^-$

PDG 2022

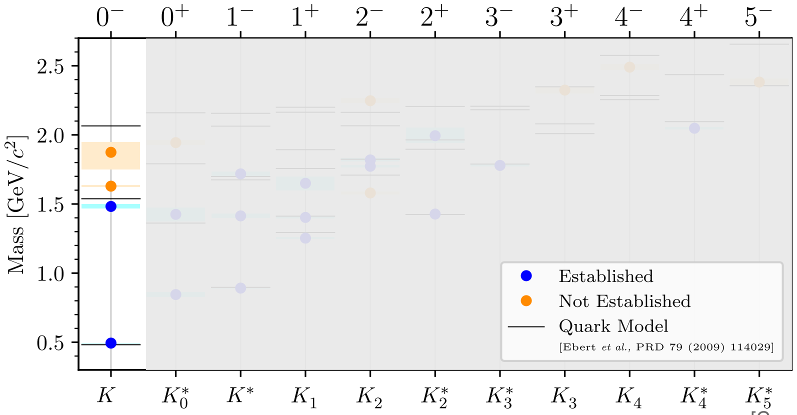

[Courtesy S. Wallner, TUM]

- $K(1460)$ is established
- $K(1630)$ and $K(1830)$ need confirmation
- $K(1630)$ seen by only one experiment
  - Width is only 16 MeV/c^2
  - Unknown J^P

Partial Waves with $J^P = 0^-$

- Peak at about 1.4 GeV/c^2 described by established $K(1460)$
  - But region $m_{K\pi\pi} \lesssim$ 1.5 GeV/c^2 affected by known analysis artifacts
  - $K(1460)$ parameters fixed to LHCb result

EPJC **78** (2018) 443

- Second peak at about 1.7 GeV/c^2
  - $K(1630)$ signal with 8.3σ statistical significance
  - Accompanied by rising phase motion
- Small bump below 2.0 GeV/c^2
  - Described by $K(1830)$ with 5.4σ statistical significance

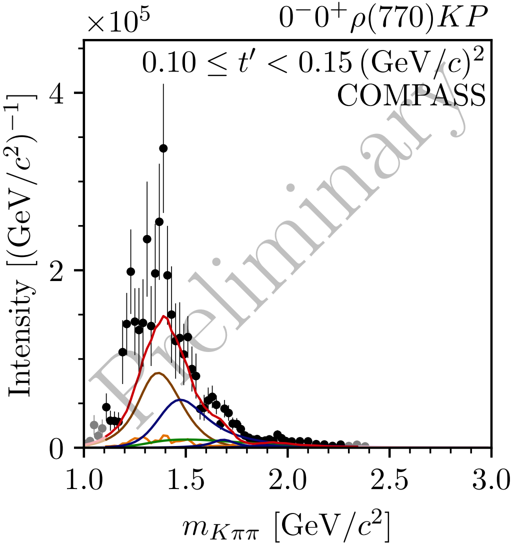

Partial Waves with $J^P = 0^-$

- Peak at about 1.4 GeV/c^2 described by established $K(1460)$
  - But region $m_{K\pi\pi} \lesssim$ 1.5 GeV/c^2 affected by known analysis artifacts
  - $K(1460)$ parameters fixed to LHCb result

EPJC **78** (2018) 443

- Second peak at about 1.7 GeV/c^2
  - $K(1630)$ signal with 8.3σ statistical significance
  - Accompanied by rising phase motion
- Small bump below 2.0 GeV/c^2
  - Described by $K(1830)$ with 5.4σ statistical significance

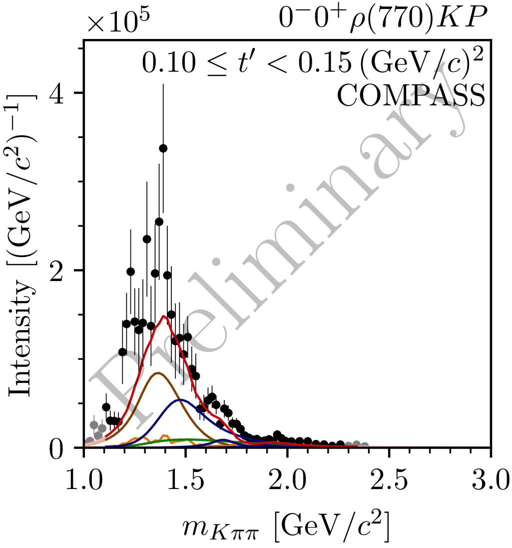

Partial Waves with $J^P = 0^-$

- Peak at about 1.4 GeV/c^2 described by established $K(1460)$
  - But region $m_{K\pi\pi} \lesssim$ 1.5 GeV/c^2 affected by known analysis artifacts
  - $K(1460)$ parameters fixed to LHCb result

EPJC **78** (2018) 443

- Second peak at about 1.7 GeV/c^2
  - $K(1630)$ signal with 8.3σ statistical significance
  - Accompanied by rising phase motion
- Small bump below 2.0 GeV/c^2
  - Described by $K(1830)$ with 5.4σ statistical significance

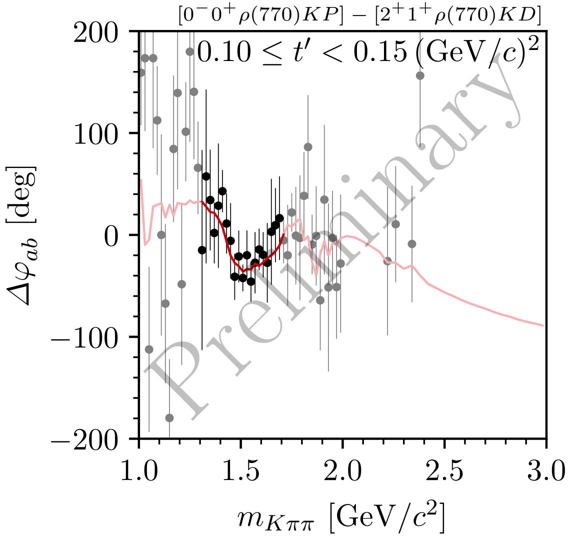

Partial Waves with $J^P = 0^-$

- Peak at about 1.4 GeV/c^2 described by established $K(1460)$
  - But region $m_{K\pi\pi} \lesssim 1.5$ GeV/c^2 affected by known analysis artifacts
  - $K(1460)$ parameters fixed to LHCb result

EPJC **78** (2018) 443

- Second peak at about 1.7 GeV/c^2
  - $K(1630)$ signal with 8.3σ statistical significance
  - Accompanied by rising phase motion
- Small bump below 2.0 GeV/c^2
  - Described by $K(1830)$ with 5.4σ statistical significance

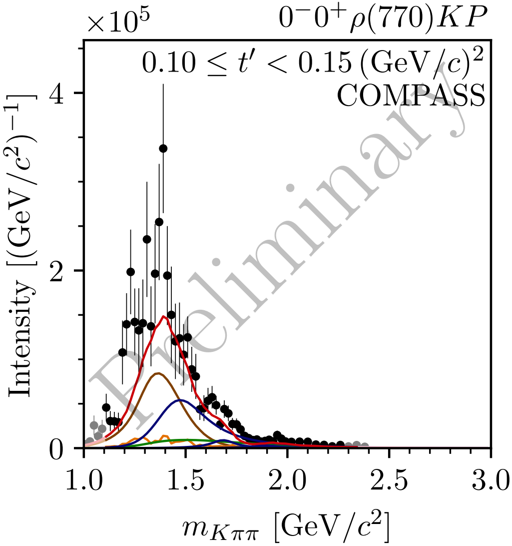

Partial Waves with $J^P = 0^-$

$K(1630)$ and $K(1830)$

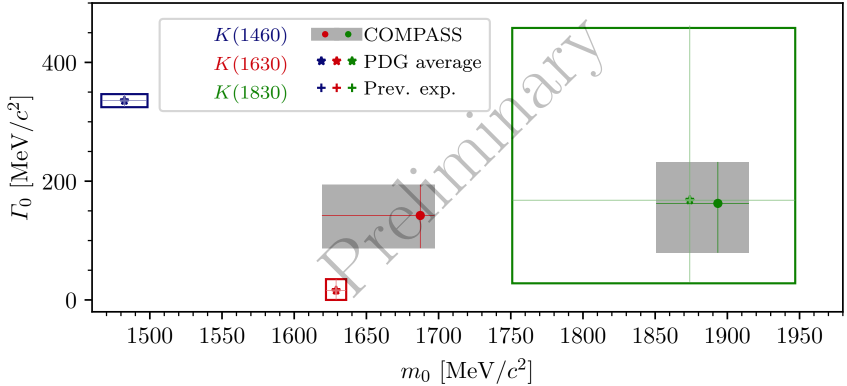

- $K(1830)$ parameters in good agreement with LHCb measurement PRL **118** (2017) 022003
- $K(1630)$:
  - Mass in agreement with previous measurement Karnaukhov *et al.*, Phys. Atom. Nucl. **61** (1998) 61
  - More reasonable width value of $\Gamma_0 = 140 \pm 20\,(\text{stat.}) \pm 50\,(\text{sys.})\ \text{MeV}/c^2$

Partial Waves with $J^P = 0^-$

$K(1630)$ and $K(1830)$

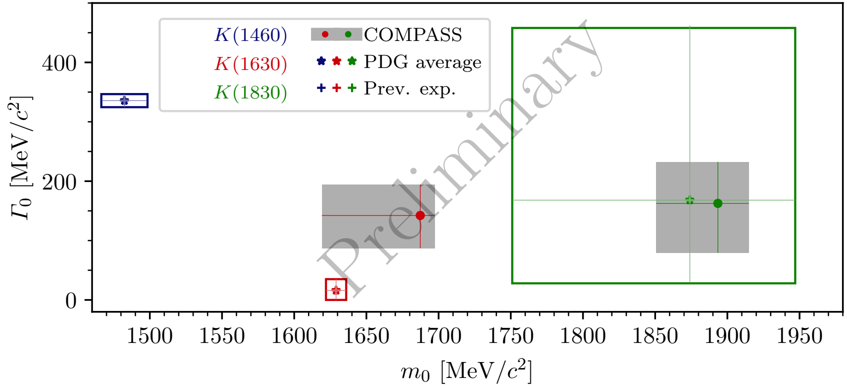

- $K(1830)$ parameters in good agreement with LHCb measurement — PRL **118** (2017) 022003
- $K(1630)$:
  - Mass in agreement with previous measurement — Karnaukhov *et al.*, Phys. Atom. Nucl. **61** (1998) 61
  - More reasonable width value of $\Gamma_0 = 140 \pm 20\,(\text{stat.}) \pm 50\,(\text{sys.})\ \text{MeV}/c^2$

Partial Waves with $J^P = 0^-$

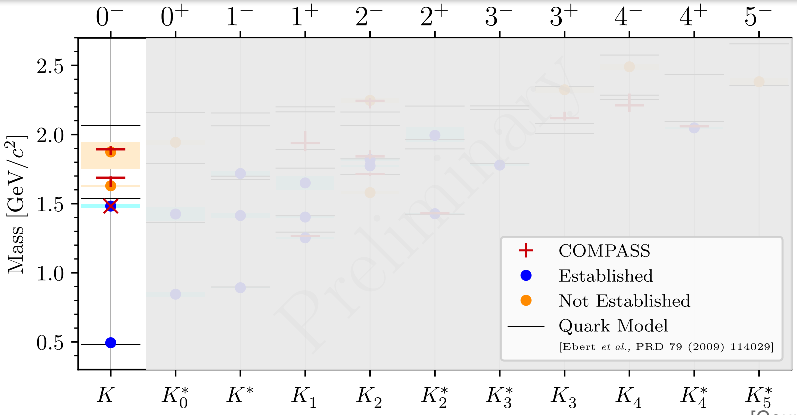

[Courtesy S. Wallner, TUM]

- Indications for 3 excited K states extracted simultaneously in a single fit
- Quark model predicts only 2 excited states in this mass region
- $K(1460)$ and $K(1830)$ are good $q\bar{q}$ candidates

Partial Waves with $J^P = 0^-$

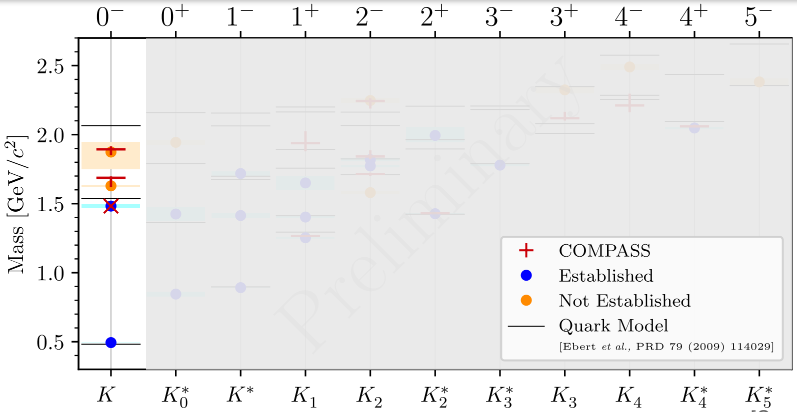

[Courtesy S. Wallner, TUM]

- $K(1630)$ is supernumerary state
- Candidate for exotic non-$q\bar{q}$ state
- But other explanations not excluded, e.g. state is close to $K^*(892)\omega(782)$ threshold

Summary

Jefferson Lab
Thomas Jefferson National Accelerator Facility

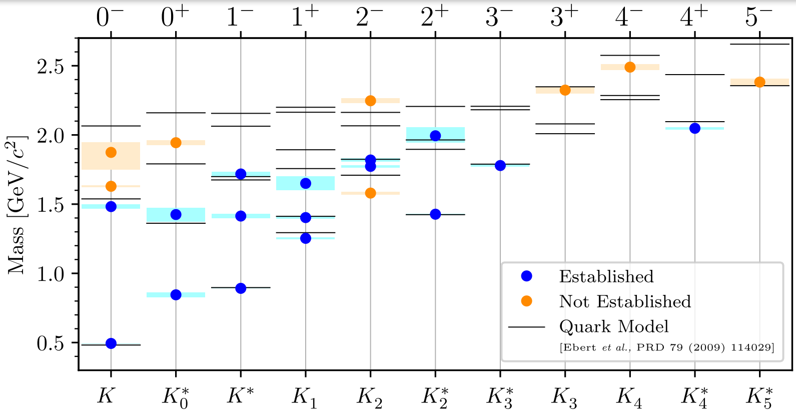

The strange-meson spectrum

- Many states require further confirmation or have not been found yet
- Search for strange partners of exotic non-strange light-mesons

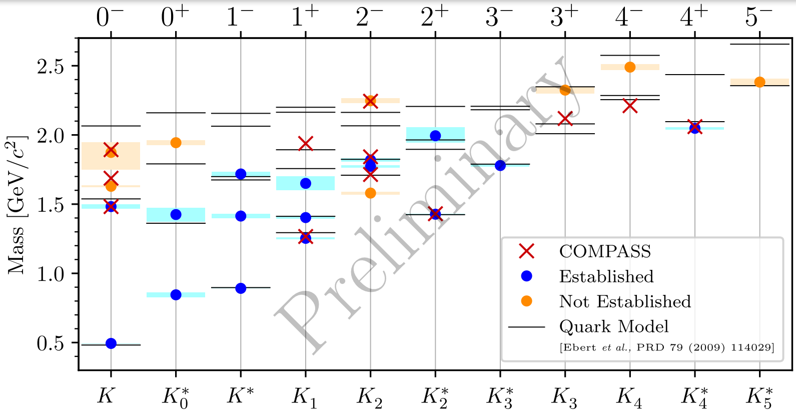

COMPASS

- Most detailed and comprehensive analysis of the $K^- \pi^- \pi^+$ final state so far
- Supernumerary kaon state with $J^P = 0^-$ $\Longrightarrow$ candidate for exotic strange meson

Summary

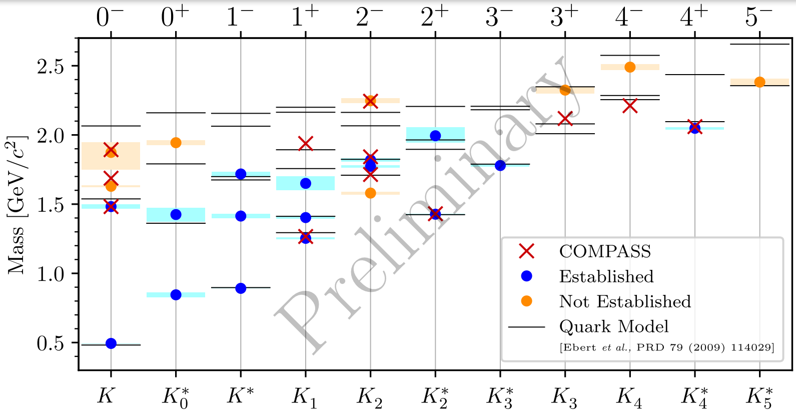

Planned experiment: AMBER at CERN

- Proposal for high-precision strange-meson spectroscopy
- *Goal:* collect 10 to 20 × 10^6 $K^-\pi^-\pi^+$ events using high-intensity high-energy kaon beam

Part II

Backup Slides

Backup Slides

5 PWA model

6 Resonance parameters

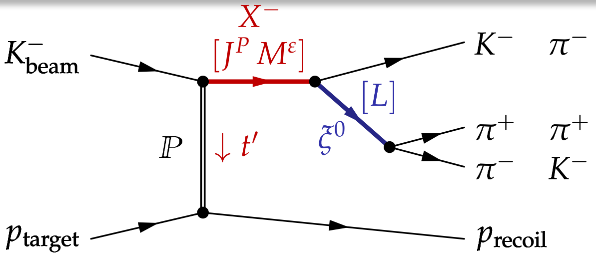

- Sum of partial-wave amplitudes
- Wave set:
  - Spin $J \leq 7$
  - Orbital angular momentum $L \leq 7$
  - Positive naturality of the exchange particle
  - 12 isobar resonances:
    - $[K\pi]_S^{K\pi}$, $[K\pi]_S^{K\eta}$, $K^*(892)$, $K_2^*(1430)$, $K^*(1680)$, $K_3^*(1780)$
    - $[\pi\pi]_S$, $f_0(980)$, $f_0(1500)$, $\rho(770)$, $f_2(1270)$, $\rho_3(1690)$

Resonances with $J^P = 1^+$

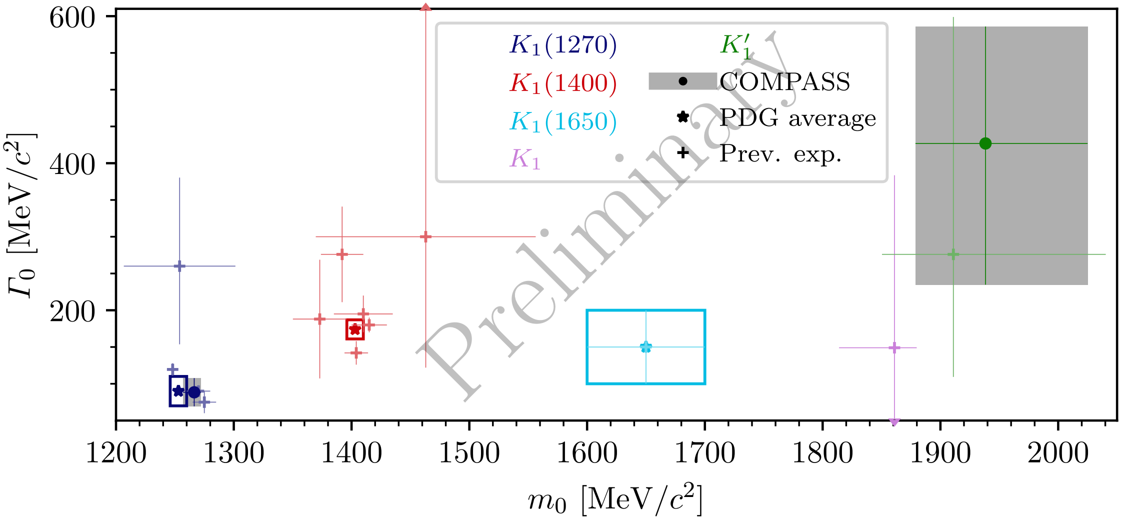

Resonances with $J^P = 2^+$

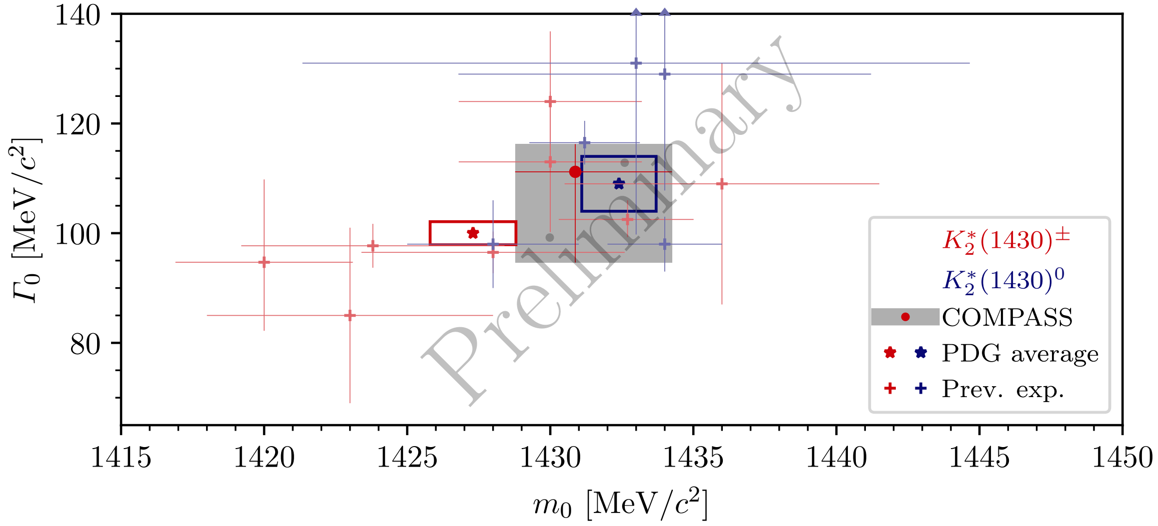

Resonances with $J^P = 3^+$

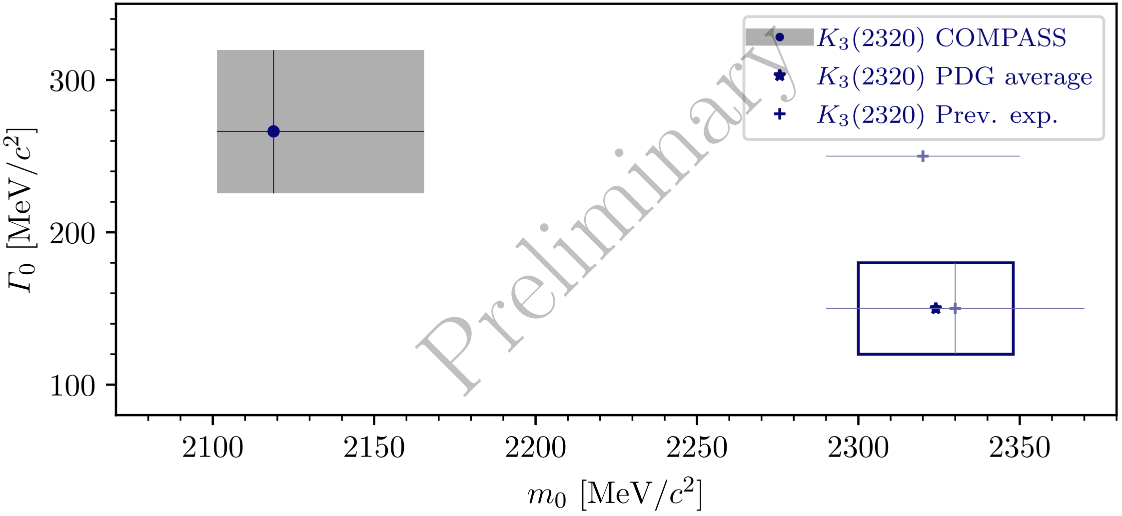

Resonances with $J^P = 4^+$

Jefferson Lab
Thomas Jefferson National Accelerator Facility

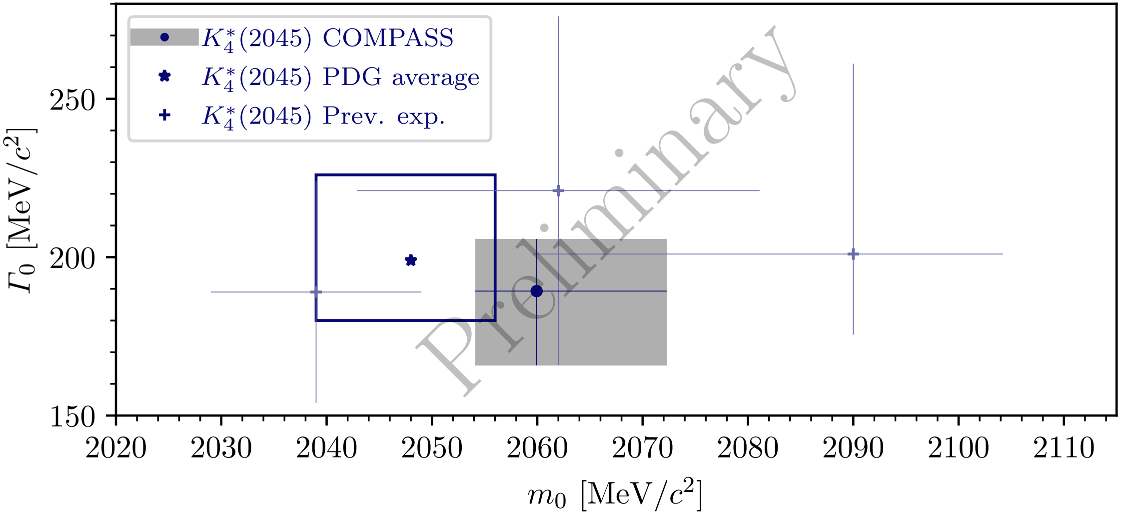

Resonances with $J^P = 4^-$